

## Invariants of Spherical Harmonics as Order Parameters in Liquids

**András Baranyai, Alfonz Geiger,<sup>†</sup> Philip R. Gartrell-Mills,<sup>‡</sup> Karl Heinzinger,\*  
Robert McGreevy,<sup>‡</sup> Gábor Pálinkás<sup>¶</sup> and Imre Ruff\***

*Laboratory of Theoretical Chemistry, Department of Chemistry, L. Eötvös University,  
Budapest, Múzeum krt. 6-8, H-1088 Hungary*

The application of the second- and third-order invariants of the even-*l* spherical harmonics for the geometrical characterization of clusters in disordered systems is discussed. Their use as sensitive order parameters is useful in the geometrical analysis of computer-simulated configurations. It is shown that the second- and third-order invariants give information on the three- and four-body angular correlations, respectively. The values of the invariants calculated for a given configuration set depend on the number of particles and their neighbours considered, *i.e.* on the size of the statistical sample. A renormalization is suggested to eliminate this size effect. By choosing a suitable method of averaging the spherical harmonics, they can be made characteristic either of the angular correlations within individual clusters only or also of cross-correlations between a set of clusters. Thus they can be used for the detection of traces of longer-range crystalline structures.

The first five even-*l* invariants have been calculated for configurations of liquid argon, molten alkali-metal halides, and pure water simulated by Monte Carlo or molecular-dynamic methods. The results indicate that the structure of the first coordination spheres in liquid argon are slightly distorted hexagonal close-packed clusters which have practically no angular correlation with one another. Nearest-neighbour angular correlations in sodium, potassium, rubidium and caesium chlorides correspond to more or less distorted face-centred cubic lattices, while LiI and LiCl resemble the wurtzite and sphalerite structure, respectively. In comparison with the above cases, water is disordered to the extent that even the distorted tetrahedral clusters are barely recognizable. Peculiarly distorted tetrahedra which are in a characteristic angular correlation with one another are stabilized by a decrease in the density of water.

---

The use of pair correlation functions is the common way of characterizing the structure of highly disordered systems such as liquids. However, since these are averages of relative radial density distributions over all particles of a kind, taken as centres, and also averages over the polar angles in each of these coordinate systems, for the description of some physical properties the pair correlation functions are sometimes not sufficiently sensitive characteristics of the fluid structure. This may be the case, for example, in the

<sup>†</sup> Institut für Physikalische Chemie, Rhein-Westfahl Technische Hochschule, Aachen, Federal Republic of Germany.

<sup>‡</sup> Clarendon Laboratory, Department of Physics, University of Oxford, Parks Road, Oxford OX1 3PU.

<sup>§</sup> Max-Planck-Institut für Chemie (Otto-Hahn-Institut), 6500 Mainz, Saarstrasse 23, Federal Republic of Germany.

<sup>¶</sup> Central Research Institute for Chemistry of the Hungarian Academy of Sciences, Budapest, Pusztaszeri út 53-67, H-1023 Hungary.

study of nucleation in phase transition, when the characteristic changes of the pair correlation function due to local order in some regions is smoothed out by the averaging over all particles. Similarly, the interpretation of physical processes, in which the asymmetry of the nearest neighbourhood is of crucial importance, would require information on the angular correlations averaged over in the purely distance-dependent pair correlation functions.

The obstacles to obtaining more detailed information about the structure of fluids seem to be less in the theoretical than in the experimental approach. Revealing many-body and/or orientational correlations within and in between clusters of atoms or molecules in liquids would need an unconventional set-up in diffraction experiments as suggested recently by Ackerson *et al.*<sup>1</sup> Their idea to evaluate the 'apertured cross-correlation function' by using two simultaneous detectors is very attractive, yet it has been utilized in real experiments only on colloid systems so far.<sup>1b</sup> Application of the technique to liquids with correlation on atomic distance scales requires further development of synchrotron X-ray sources.

Considering the theoretical approach, the adequate description of more complex correlations in computer-simulated sets of configurations seems promising. Extensive work has been carried out recently by Stillinger and coworkers<sup>2-9</sup> in search for the 'inherent liquid structure'. This can be obtained during molecular-dynamics simulations by quenching the system from time to time, suddenly diminishing the kinetic energy of the particles and positioning them in the local potential-energy minima. The pair correlation functions calculated for such quenched states reveal more of the fundamental liquid structure undisturbed by (strongly anharmonic) atomic vibrations. As a consequence of the sharpening of the peaks in these pair correlation functions, the onset of eventual nucleation in freezing or condensation is sensitively signalled by the appearance of small peaks characteristic of the new phase.

While the 'sensitization' of the pair correlation function by quenching is a useful idea, it is more difficult to find an economic and relatively simple method to characterize local angular correlations. With this aim some papers have been published on the application of Dirichlet-Voronoi (DV) polyhedra<sup>10-11</sup> (or, as they are sometimes called, Wigner-Seitz cells).<sup>12-19</sup> It is disappointing that the statistical geometrical information carried by them cannot be handled in a simple mathematical way; instead the distribution functions of their various features must be studied. Nevertheless, the DV polyhedra are unequivocal descriptions of the configurations, and their calculation does not require much computer time.

Many-body correlation functions are often expanded into series using the complete orthogonal system of the spherical harmonics. This approach, while convenient in the theory of liquids based on integral equations, is not economic for the characterization of simulated configurations. Also, the higher-order terms of these series are themselves complicated, which does not facilitate the visualization of their physical meaning.

Instead of the full expansion of the many-body correlation functions, Steinhardt *et al.*<sup>20</sup> revived Landau's suggestion<sup>21</sup> of the use of the second- and third-order rotational invariants of even- $l$  spherical harmonics. In simplified form they can be applied to characterize only the angular correlations in a given (simulated) configuration of the system. They have proved to be sensitive order parameters for indicating phase transitions<sup>22</sup> or distinguishing between geometrical alternatives of coordination spheres.<sup>23</sup> However, as with many fruitful ideas, their first applications were not executed in the most convenient way.

In the next section we give a detailed survey of what is characterized by the invariants of spherical harmonics, both in the form suggested by Steinhardt *et al.* and in a modified version first used in ref. (23). Their applications to some fundamental types of liquids will be discussed in the subsequent sections, *viz.* for a Lennard-Jones liquid, for molten alkali-metal halides and for water. By comparing the results for these fluids, some

conclusions can be obtained on the conditions regulating the sensitivity of the spherical-harmonic invariants to the geometrical structure of the system.

### Spherical Harmonics and their Rotational Invariants

In common computer simulations the periodic boundary conditions are fulfilled by the translations of the cube containing the particles in all directions. Thus the configurations are given by the atomic coordinates in the reference frame of the simulation box. Since the comparison of local angular correlations in molecular clusters of some size can be studied only in local coordinate systems which, from the point of view of comparison, are properly rotated with respect to one another, an efficient mathematical method is required for either the 'alignment' of the clusters to be compared or for the characterization of the angular correlations by rotationally invariant parameters.

The idea of Steinhardt *et al.*<sup>20</sup> was to use the rotational invariants of the even- $l$  spherical harmonics. These invariants are as follows:

$$Q = \left( \frac{4\pi}{2l+1} \sum_{m=-l}^l |Q_{lm}|^2 \right)^{1/2} \quad (1)$$

and

$$W_l = \sum_{\substack{m_1, m_2, m_3 \\ m_1 + m_2 + m_3 = 0}} \begin{vmatrix} l & l & l \\ m & m_2 & m_3 \end{vmatrix} Q_{lm_1} Q_{lm_2} Q_{lm_3} \quad (2)$$

respectively, where

$$Q_{lm} = \langle Y_{lm}(\theta, \phi) \rangle \quad (3)$$

in which  $Y_{lm}(\theta, \phi)$  are the spherical harmonics of the polar angles of a vector pointing from a particle considered to be central in a cluster to one of its neighbours within the cluster. In principle, a cluster may be any finite set of the particles comprising the liquid. In practice they can be limited only to a given number of nearest neighbours or to the neighbours within a pre-set cut-off sphere or to Voronoi neighbours.<sup>19</sup>

The mean value indicated in eqn (3) is taken over all such vectors in a system, irrespective of whether they belong to the same cluster or not.

Just as the angular momentum quantum number,  $l$ , is a characteristic quantity of the 'shape' of an atomic orbital, the quantity  $Q_l$  is a rotationally invariant characteristic value of the shape of a given cluster (if the average is taken only over bonds within a given cluster) or an average of such values for a set of clusters. Therefore, the choice of the directions  $\theta = 0$  and  $\phi = 0$  is quite arbitrary, and so for the sake of convenience they can be adjusted to the coordinate system of the simulation box.

The multiplier of the  $Q_{lm}$  in eqn (2) is the so-called Wigner  $3j$  symbol,<sup>24</sup> and with this normalization the quantity  $W_l$  is another rotationally invariant characteristic of the cluster geometry.

### Geometrical Information in the $Q_l$

In order to clarify the geometrical implications of the invariants, let us write eqn (1) in detailed form as follows:

$$Q_l^2 = \frac{4\pi}{2l+1} \sum_{m=-l}^l \sum_{i=1}^{N_b} \sum_{j=1}^{N_b} P_l^{|m|}(\cos \theta_i) P_l^{|m|}(\cos \theta_j) \times \cos[m(\phi_i + \phi_j)] \quad (4)$$

where  $P_l^{|m|}(x)$  is the associated Legendre polynomial, and we have utilized the Euler form of complex numbers. In this case we can safely reverse the order of summation, so that after the sums with respect to  $i$  and  $j$  we find exactly the superposition theorem

of the spherical harmonics.<sup>25</sup> Thus we have

$$Q_l^2 = \left( \sum_{i,j} P_l(\cos \omega_{ij}) \right) / N_b^2 \quad (5)$$

where  $N_b$  is the number of bonds considered. Since  $\cos(\omega_{ij}) = 1$  if  $i = j$ , we have

$$Q_l^2 = 1/N_b + 2 \sum_{\substack{i,j \\ i < j}} P_l(\cos \omega_{ij}) / N_b^2 \quad (6)$$

where  $P_l(x)$  is the common (not associated) Legendre polynomial.

Thus the  $Q_l$  characterize the distribution of the cosines of angles formed by any pair of bond vectors. This form of the  $Q_l$  is especially suitable for illustrating features not sufficiently emphasized in the paper of Steinhardt *et al.*<sup>20</sup>

(i) The averaging procedure in eqn (3) yields positive definites for the  $Q_l$  either if there is some translational symmetry regulating the 'alignment' of the clusters (*i.e.* the system is a more or less disordered lattice) or if the orientation of the clusters is completely random but the system is finite. Or, in a complementary formulation of this statement, the  $Q_l$  ( $l > 0$ ) are always zero for an infinite isotropic system.

(ii) Partly as a consequence of this, the second-order invariants, except  $Q_0$  which is always unity, depend on the number of bonds considered in a sample [see eqn (6)] if the configurations are not ideally crystalline. This is so, since the integral of the Legendre polynomials are zero in the range  $-1$  to  $+1$ , and therefore any subset of  $\cos \omega_{ij}$  that correspond to a random distribution would not contribute to the sum (just as odd- $l$  spherical harmonics would not as far as the system is isotropic). Thus, if the distribution of the polar angles is not infinitely dense in a finite, but highly disordered, system, the even- $l$   $Q_{lm}$  will never be zero, but some positive definites.

(iii) From this latter property it follows that comparisons between sets of  $Q_l$  obtained for different samples should be made only when the number of bonds is the same in each case considered or when a suitable renormalization has been carried out. In this paper we normalize the  $Q_l$  so that in the corresponding perfectly random case they would be unity for all even  $l$ .

(iv) From eqn (4) it is also obvious that the second-order rotational invariants characterize three-body angular distributions.

We mention in passing that it is more economic to use eqn (1) and (3) rather than eqn (6) to evaluate the  $Q_l$  for a set of bonds between a few hundred particles. Although the calculation of spherical harmonics is more cumbersome than that of Legendre polynomials, from a certain number of bonds upwards, the number of pairs in the sum of eqn (6) becomes so large that it overcompensates the gain given by the more simple formulae.

The procedure suggested by Steinhardt *et al.* for averaging the spherical harmonics makes the invariants involve angular correlations within the clusters as well as cross-correlations in between them. If we break down the procedure into two, *viz.* first averaging within the clusters, then calculating the invariants, and finally averaging them, they would carry information only on angular correlations within the clusters. Obviously the two kinds of averages would become identical in the two extreme cases: (a) if the clusters were rotated in the liquid with respect to one another in a perfectly random way (because the inter-cluster correlations would vanish) and (b) if the system were an ideal crystal lattice (because intra- and inter-cluster pairs of bonds would then form the same angles). Real liquids can be expected more to resemble case (a).

### Geometrical Information in the $W_l$

The geometrical implications of the third-order rotational invariants are similar to those of the second-order ones in that they characterize the distribution of the three angles

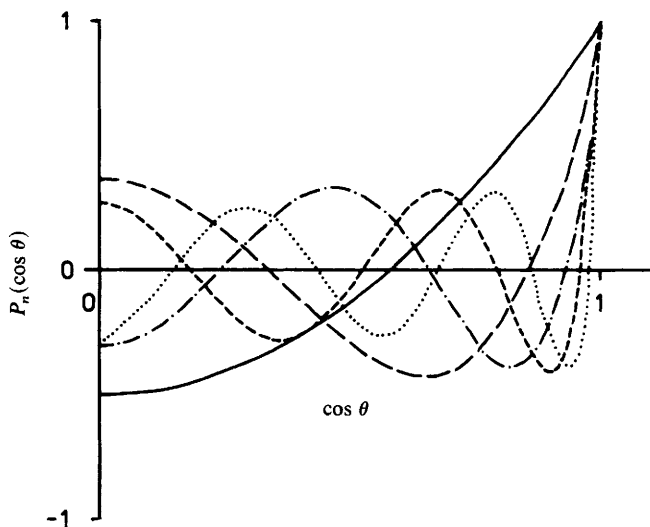


Fig. 1. The first five even- $l$  Legendre polynomials. (—)  $n=2$ , (---)  $n=4$ , (-·-)  $n=6$ , (····)  $n=8$ , (·····)  $n=10$ .

formed by any two bond vectors joining particles within or in between the clusters. Thus they are characteristic of the four-body angular correlations.

In order to show this in more detail, let us transcribe eqn (2) into the following form:

$$\begin{aligned}
 W_l = & \sum_{\substack{m_1, m_2, m_3 \\ m+m_2+m_3=0}} \begin{vmatrix} l & l & l \\ m_1 & m_2 & m_3 \end{vmatrix} \\
 & \times \sum_{r=1}^{N_b} \sum_{s=1}^{N_b} \sum_{t=1}^{N_b} P_l^{|m_1|}(\cos \theta_r) P_l^{|m_2|}(\cos \theta_s) P_l^{|m_3|}(\cos \theta_t) \\
 & \times \cos |m_1(\phi_r - \phi_t) + m_2(\phi_s - \phi_t)|
 \end{aligned} \quad (7)$$

where we have utilized the property of the three sums (each over all angles) to eliminate the imaginary part of the  $\phi$ -dependence, which cancels due to the antisymmetry of the sine function, and the condition of the first summation to eliminate  $m_3$  from the argument of the cosine factors. This formula shows clearly that (a) the  $W_l$  indeed characterize the three-angle (*i.e.* four-body) correlation, (b) they are real numbers just as the  $Q_b$ , and (c) they depend on the angles formed between pairs of bond vectors.

Since the increase in sample size also diminishes the  $W_l$  some kind of normalization must be applied to these values as well. This can be made according to the suggestion of Steinhardt *et al.*,<sup>20</sup> who define the ratio of the third- and second-order invariants as follows:

$$w_l = W_l / \left| \frac{2l+1}{4\pi} Q_l^2 \right|^{3/2} \quad (8)$$

where  $Q_l$  now means the renormalized second-order invariant.

From eqn (7) it is evident that the calculation of the  $w_l$  is more expensive than that of  $Q_l$  which itself requires considerable computer time. This fact imposes an upper limit on  $l$ . There is, however, an additional, more academic, reason why the higher even- $l$  invariants are not worth calculating. Namely, when the average period of the oscillations of the Legendre polynomial (see fig. 1) in the  $\cos \omega_{ij}$  space becomes smaller than the scattering of some characteristic angle, the corresponding invariant would

rapidly vanish. For the actual samples studied in this paper  $l \leq 10$  proved to be sufficient, as suggested by Steinhardt *et al.*

### Reference Sets of Invariants for Various Cluster Geometries

The equations given previously determine a unique set of the even- $l$  invariants for a given configuration of the fluid. Unfortunately, the solution of the inverse problem, *viz.* the calculation of the average polyhedron corresponding to the more or less characteristic geometry of the clusters, is not definite.

Thus, while sets of  $Q_l$  and  $w_l$  may be extremely useful as order parameters, they are less unanimously informative when the actual structure is sought.

The only practical way of geometrical analysis is to calculate a reference set of the rotational invariants for clusters including different numbers of particles with various geometries, and find the most reasonable (but not unique) average geometry by the best fit to the values obtained for a simulated configuration. For this purpose we have calculated the invariants for various, gradually randomized,  $N$ -neighbour clusters of a central particle.

The randomization was carried out by displacing the neighbours according to a normal distribution applied in the  $x$ ,  $y$  and  $z$  directions. In the original, regular, arrangements the neighbouring particles were placed onto the surface of a unit sphere. The standard deviation of the normal distribution was set to the same value in all three directions and measured relative to the unit particle distance assumed.

According to the two different ways of averaging the spherical harmonics over the bonds, we have calculated two reference sets as follows. In one, which we shall call 'the distorted lattice case', the gradual randomization was carried out on clusters originally oriented in the same direction, *i.e.* preserving more or less of the translational symmetry of a lattice, and the mean value in eqn (3) was obtained for all bonds irrespective of whether they belong to the same cluster or to two different ones. In the other, 'the individual cluster case', averages of spherical harmonics were taken only within each cluster, and then the invariants themselves were averaged. This is equivalent to handling the same set of clusters as those in the distorted lattice case as if rotated at random with respect to one another.

Excerpts of these reference sets are given in tables 1 and 2. [Two technical comments to be noted are as follows. (1) The  $w_l$  of the individual cluster case converge so rapidly to zero that it is not worth while listing them. (2) Some smaller clusters given in table 2 have been omitted from table 1, since a reasonable lattice-like structure constructed from them would require not only translation but also definite rotations. If, for some reason, such cases were to be calculated, one should rather define a larger basic cluster involving the rotated versions and still consider translational replicas only.] As expected, the differences between the two sets are considerable. A general feature of the differences is that the same scattering of the position coordinates causes slower convergence to unity in the  $Q_l$  of the distorted lattice than in the individual cluster case. Another general trend is that the  $Q_2$  are usually larger for the lattice which is the consequence of originally parallel bonds forming angles close to zero owing to gradual randomization.

The distribution of the cosine of angles between pairs of bonds in the individual clusters has also been calculated. Fig. 2 offers some of these distributions for comparison. Whereas, with a mean square deviation of *ca.* 0.3 of the randomization, the noise of the cosine distributions makes different geometries indistinguishable, some of the corresponding  $Q_l$  of table 2 still differ from unity beyond statistical error. This demonstrates the sensitivity of the invariants as order parameters.

For the comparison of the second- and third-order invariants calculated for sets of simulated configurations with these reference values we used a computer program which

**Table 1.** Second- and third-order invariants of even- $l$  spherical harmonics for various cluster geometries and their random distortions ('distorted lattice' case)

randomization degree	1	$Q_1$	$w_1 \times 10^5$	normalization factor for 20 clusters
diamond-4 (tetrahedron)				
0	2	0.009	-1541	2.494
	4	1.269	-1027	
	6	1.567	84	
	8	0.531	377	
	10	1.621	-581	
0.1	2	0.102	254	3.175
	4	1.479	-481	
	6	1.646	33	
	8	0.533	128	
	10	1.237	-261	
0.2	2	0.384	0	4.911
	4	1.673	-126	
	6	1.451	9	
	8	0.637	-15	
	10	0.852	-17	
0.3	2	0.725	8	5.880
	4	1.525	-61	
	6	1.099	-20	
	8	0.839	16	
	10	0.810	-2	
0.4	2	1.021	-12	8.334
	4	1.157	4	
	6	0.942	3	
	8	1.029	3	
	10	0.848	-1	
square planar-4				
0	2	0.751	7044	1.502
	4	1.245	3683	
	6	0.881	-213	
	8	1.199	1880	
	10	0.922	-481	
0.1	2	0.915	3614	1.875
	4	1.413	1910	
	6	0.916	-101	
	8	1.056	982	
	10	0.697	-221	
0.2	2	1.411	759	3.132
	4	1.739	407	
	6	0.877	-18	
	8	0.621	142	
	10	0.350	26	

## Order Parameters in Liquids

Table 1. (continued)

randomization degree	1	$Q_1$	$w_1 \times 10^5$	normalization factor for 20 clusters
0.3	2	1.691	225	4.655
	4	1.499	112	
	6	0.685	17	
	8	0.600	14	
	10	0.522	-11	
0.4	2	1.744	145	5.342
	4	1.104	60	
	6	0.591	3	
	8	0.879	4	
	10	0.679	0	
face-centred cubic-6				
0	2	0	0	2.225
	4	1.699	1445	
	6	0.786	119	
	8	1.597	530	
	10	0.915	817	
0.1	2	0.027	-5	2.521
	4	1.750	990	
	6	0.731	82	
	8	1.633	321	
	10	0.857	116	
0.2	2	0.235	18	4.781
	4	2.352	142	
	6	0.744	23	
	8	0.828	20	
	10	0.839	-4	
0.3	2	0.644	1	5.721
	4	2.040	82	
	6	0.677	11	
	8	0.681	0	
	10	0.956	1	
0.4	2	0.547	6	8.169
	4	1.718	20	
	6	0.872	2	
	8	0.677	-3	
	10	1.184	-1	
body-centred cubic-8				
0	2	0	0	2.494
	4	1.269	-1027	
	6	1.567	84	
	8	0.531	377	
	10	1.621	-581	
0.1	2	0.040	447	3.231
	4	1.496	-467	
	6	1.666	37	
	8	0.509	146	
	10	1.287	-252	



Table 1. (continued)

randomization degree	1	$Q_1$	$w_1 \times 10^5$	normalization factor for 20 clusters
0.2	2	0.270	39	5.682
	4	2.002	-77	
	6	1.662	5	
	8	0.477	2	
	10	0.586	-18	
0.3	2	0.318	-1	8.982
	4	2.163	-21	
	6	1.255	1	
	8	0.505	-1	
	10	0.756	0	
0.4	2	0.942	-6	11.638
	4	1.295	-7	
	6	1.014	1	
	8	0.772	-2	
	10	0.974	-1	
icosahedron-12				
0	2	0	0	4.868
	4	0	-31	
	6	3.229	-148	
	8	0	3	
	10	1.770	-81	
0.1	2	0.097	-138	5.035
	4	0.176	56	
	6	2.647	-132	
	8	0.631	2	
	10	1.448	-14	
0.2	2	0.169	17	9.059
	4	0.335	2	
	6	2.888	-22	
	8	0.822	1	
	10	0.785	-4	
0.3	2	0.611	2	14.132
	4	0.723	0	
	6	1.845	-4	
	8	0.799	-1	
	10	1.019	-1	
0.4	2	0.823	-1	13.231
	4	0.969	1	
	6	1.510	-1	
	8	0.893	-1	
	10	0.803	-1	
face-centred cubic-12				
0	2	0	0	4.229
	4	0.807	-211	
	6	2.429	-18	
	8	1.708	77	
	10	0.054	-120	

Table 1. (continued)

randomization degree	1	$Q_1$	$w_1 \times 10^5$	normalization factor for 20 clusters
0.1	2	0.246	0	4.905
	4	0.878	-127	
	6	2.229	-12	
	8	1.372	47	
	10	0.273	3	
0.2	2	0.358	-2	8.066
	4	1.169	-21	
	6	2.004	-3	
	8	0.994	6	
	10	0.472	1	
0.3	2	0.730	2	13.338
	4	1.078	-2	
	6	1.457	0	
	8	0.678	-1	
	10	1.054	0	
0.4	2	0.650	-1	14.960
	4	0.723	-2	
	6	0.857	-2	
	8	1.586	-1	
	10	1.182	1	
hexagonal close packed-12				
0	2	0	0	5.499
	4	0.534	80	
	6	2.665	-8	
	8	1.743	30	
	10	0.055	-48	
0.1	2	0.126	2	6.428
	4	0.674	40	
	6	2.553	-5	
	8	1.335	13	
	10	0.310	-7	
0.2	2	0.400	5	10.760
	4	0.844	4	
	6	2.199	0	
	8	0.935	-1	
	10	0.621	0	
0.3	2	0.486	1	13.789
	4	0.879	-1	
	6	1.732	-1	
	8	1.116	0	
	10	0.787	0	
0.4	2	0.681	4	13.056
	4	1.154	2	
	6	1.243	1	
	8	1.030	0	
	10	0.889	-1	

Table 1. (continued)

randomization degree	1	$Q_1$	$w_1 \times 10^5$	normalization factor for 20 clusters
body-centred cubic-14				
0	2	0	0	4.259
	4	0.155	205	
	6	2.175	17	
	8	1.828	75	
	10	0.831	-117	
0.1	2	0.091	-37	4.580
	4	0.204	71	
	6	1.928	13	
	8	1.556	58	
	10	1.218	-25	
0.2	2	0.275	-29	9.068
	4	0.411	16	
	6	1.959	1	
	8	1.165	7	
	10	1.187	0	
0.3	2	0.493	1	15.136
	4	0.604	0	
	6	1.379	0	
	8	1.268	0	
	10	1.254	-1	
0.4	2	0.674	0	18.805
	4	1.017	-1	
	6	1.226	-1	
	8	0.966	-1	
	10	1.114	-1	
face-centred cubic-18				
0	2	0	0	4.856
	4	0.618	139	
	6	1.287	-11	
	8	2.469	51	
	10	0.624	79	
0.1	2	0.189	-9	5.743
	4	0.655	80	
	6	1.244	-7	
	8	2.137	29	
	10	0.773	6	
0.2	2	0.315	-1	8.731
	4	0.888	13	
	6	1.258	-2	
	8	1.427	4	
	10	1.110	0	
0.3	2	0.674	-2	14.774
	4	0.975	0	
	6	1.089	0	

Table 1. (continued)

randomization degree	1	$Q_1$	$w_1 \times 10^3$	normalization factor for 20 clusters
0.4	8	1.190	1	17.963
	10	1.071	0	
	2	0.654	-2	
	4	1.014	1	
	6	1.090	0	
	8	1.162	0	
	10	1.078	0	
0	cluster in fig. 6			
	2	0.814	-255	4.541
	4	0.684	143	
	6	1.881	-3	
	8	0.724	-29	
10	0.895	6		
<sup>a</sup>				

<sup>a</sup> Omissions due to limitations in size.

measured the goodness of the fits by taking into account the error bars on the data as well as the differences in the mean values.

### Distance Correlation between Bond Angles

The orientational correlation between clusters (identical in any other aspects) can be characterized, in principle, by their distance and by the Euler angles by which they are rotated to one another. However, once the spherical harmonics are calculated in the coordinate system of the simulation box, the following correlation function can be used with the same purpose:

$$G_l(r) = \frac{4\pi}{2l+1} \sum_{m=-l}^l \langle Y_{lm}(\mathbf{r}_1) Y_{lm}(\mathbf{r}_2) \rangle / G_0(r) \quad (9)$$

where

$$G_0(r) = 4\pi \langle Y_{00}(\mathbf{r}_1) Y_{00}(\mathbf{r}_2) \rangle. \quad (10)$$

Here  $r = |\mathbf{r}_1 - \mathbf{r}_2|$  is the distance between the mid-points of two bonds at  $\mathbf{r}_1$  and  $\mathbf{r}_2$ , and the mean values are calculated for all bonds at a distance  $r$  from one another. Eqn (11) gives the normalization factor, i.e.  $G_0(r)$  is the bond density correlation function at distance  $r$ .

If the decay of  $G_l(r)$  extends beyond the first-neighbour distance of the clusters, the latter are twisted with respect to one another by angles which do not correspond to zeros of the given spherical harmonic. If none of the  $G_l(r)$  is such, the clusters are oriented perfectly at random. On the other hand, if all of the  $G_l(r)$  decay beyond the first-neighbour distance, the clusters are arranged in parallel.

In order to eliminate the noise of the  $G_l(r)$  functions, they may be Fourier-transformed back and forth for smoothing as suggested in ref. (20).

**Table 2.** Second- and third-order invariants of even- $l$  spherical harmonics for various cluster geometries and their random distortions ('independent cluster' case)

mean square deviation	$l$	$Q_l$	normalization factor for 20 clusters
diamond-2			
0	2	0.833	1.449
	4	1.036	
	6	1.115	
	8	0.876	
	10	1.139	
diamond-3			
0	2	0.620	1.862
	4	1.088	
	6	1.266	
	8	0.724	
	10	1.299	
diamond-4			
0	2	0	2.494
	4	1.269	
	6	1.567	
	8	0.531	
	10	1.621	
0.1	2	0.258	2.345
	4	1.169	
	6	1.377	
	8	0.894	
	10	1.299	
0.2	2	0.416	2.274
	4	1.117	
	6	1.250	
	8	1.024	
	10	1.190	
0.3	2	0.559	2.222
	4	1.145	
	6	1.089	
	8	1.117	
	10	1.088	
0.4	2	0.730	2.115
	4	1.033	
	6	1.073	
	8	1.048	
	10	1.113	
diamond-5			
0	2	0.504	2.541
	4	0.881	
	6	1.432	
	8	0.698	
	10	1.482	

## Order Parameters in Liquids

Table 2. (continued)

mean square deviation	$l$	$Q_l$	normalization factor for 20 clusters
diamond-6 (symmetric)			
0	2	0.760	2.288
	4	0.750	
	6	1.297	
	8	0.857	
	10	1.334	
0.1	2	0.777	2.380
	4	0.863	
	6	1.205	
	8	0.978	
	10	1.175	
0.2	2	0.844	2.577
	4	0.946	
	6	1.118	
	8	1.011	
	10	1.078	
0.3	2	0.947	2.530
	4	1.008	
	6	0.968	
	8	1.088	
	10	0.986	
0.4	2	0.941	2.541
	4	1.034	
	6	0.964	
	8	1.052	
	10	1.006	
diamond-16			
0	2	0.425	4.590
	4	0.608	
	6	1.750	
	8	0.714	
	10	1.500	
0.1	2	0.510	4.643
	4	0.638	
	6	1.562	
	8	1.017	
	10	1.271	
0.2	2	0.599	4.694
	4	0.791	
	6	1.335	
	8	1.148	
	10	1.124	
0.3	2	0.719	4.427
	4	0.939	
	6	1.126	
	8	1.129	
	10	1.085	

Table 2. (continued)

mean square deviation	$l$	$Q_l$	normalization factor for 20 clusters
0.4	2	0.887	4.324
	4	1.026	
	6	1.005	
	8	1.024	
	10	1.056	
square planar-4			
0	2	0.751	1.502
	4	1.245	
	6	0.881	
	8	1.199	
	10	0.922	
0.1	2	0.832	1.676
	4	1.306	
	6	0.909	
	8	1.095	
	10	0.855	
0.2	2	0.927	1.918
	4	1.231	
	6	0.964	
	8	0.953	
	10	0.922	
0.3	2	0.916	2.017
	4	1.099	
	6	1.016	
	8	0.964	
	10	1.002	
0.4	2	0.993	2.047
	4	1.045	
	6	0.963	
	8	0.989	
	10	1.007	
face-centred cubic-4			
0	2	0.469	1.877
	4	1.465	
	6	0.795	
	8	1.386	
	10	0.882	
face-centred cubic-5			
0	2	0.391	1.956
	4	1.515	
	6	0.782	
	8	1.430	
	10	0.880	

## Order Parameters in Liquids

Table 2. (continued)

mean square deviation	$l$	$Q_l$	normalization factor for 20 clusters
face-centred cubic-6 <sup>a</sup>			
0	2	0	2.225
	4	1.699	
	6	0.786	
	8	1.597	
	10	0.915	
0.1	2	0.221	2.293
	4	1.633	
	6	0.869	
	8	1.328	
	10	0.947	
0.2	2	0.480	2.526
	4	1.438	
	6	1.015	
	8	1.039	
	10	1.025	
0.3	2	0.603	2.499
	4	1.200	
	6	1.026	
	8	1.106	
	10	1.063	
0.4	2	0.787	2.531
	4	1.097	
	6	1.050	
	8	1.055	
	10	1.008	
face-centred cubic-12			
0	2	0	4.229
	4	0.807	
	6	2.429	
	8	1.708	
	10	0.0546	
0.1	2	0.253	3.688
	4	0.787	
	6	1.810	
	8	1.282	
	10	0.865	
0.2	2	0.469	3.867
	4	0.950	
	6	1.378	
	8	1.140	
	10	1.062	
0.3	2	0.776	3.771
	4	0.918	
	6	1.130	
	8	1.131	
	10	1.044	



Table 2. (continued)

mean square deviation	$l$	$Q_l$	normalization factor for 20 clusters
0.4	2	0.641	3.700
	4	1.044	
	6	1.127	
	8	1.028	
	10	1.157	
face-centred cubic-18			
0	2	0	4.855
	4	0.618	
	6	1.287	
	8	2.469	
	10	0.624	
0.1	2	0.212	4.858
	4	0.734	
	6	1.218	
	8	1.905	
	10	0.929	
body-centred cubic 8			
0	2	0	2.494
	4	1.269	
	6	1.567	
	8	0.531	
	10	1.621	
0.1	2	0.127	2.724
	4	1.348	
	6	1.468	
	8	0.761	
	10	1.295	
0.2	2	0.419	3.040
	4	1.311	
	6	1.239	
	8	0.940	
	10	1.087	
0.3	2	0.675	3.063
	4	1.138	
	6	1.054	
	8	1.075	
	10	1.056	
0.4	2	0.613	3.091
	4	1.117	
	6	1.108	
	8	1.102	
	10	1.058	

## Order Parameters in Liquids

Table 2. (continued)

mean square deviation	$l$	$Q_l$	normalization factor for 20 clusters
body-centered cubic-14			
0	2	0	4.259
	4	0.155	
	6	2.175	
	8	1.828	
	10	0.831	
0.1	2	0.356	4.057
	4	0.376	
	6	1.827	
	8	1.443	
	10	0.995	
0.2	2	0.398	4.349
	4	0.843	
	8	1.166	
	10	1.160	
0.3	2	0.687	4.336
	4	0.963	
	6	1.114	
	8	1.100	
	10	1.134	
0.4	2	0.777	4.103
	4	1.070	
	6	1.061	
	8	0.980	
	10	1.110	
trigonal planar-3			
0	2	0.959	1.919
	4	0.719	
	6	1.422	
	8	1.023	
	10	0.875	
	<sup>a</sup>		
trigonal pyramid-4			
0	2	0.308	2.468
	4	1.311	
	6	1.244	
	8	1.407	
	10	0.728	
	<sup>a</sup>		
trigonal bipyramid-5			
0	2	0.232	2.326
	4	1.453	
	6	1.059	
	8	1.459	
	10	0.794	
	<sup>a</sup>		

Table 2. (continued)

mean square deviation	$l$	$Q_l$	normalization factor for 20 clusters
hexagonal close packed-12			
0	2	0	5.499
	4	0.534	
	6	2.665	
	8	1.743	
	10	0.055	
0.1	2	0.338	4.491
	4	0.483	
	6	1.903	
	8	1.304	
	10	0.970	
0.2	2	0.672	4.106
	4	0.672	
	6	1.332	
	8	1.214	
	10	1.108	
0.3	2	0.660	3.918
	4	1.025	
	6	1.140	
	8	1.066	
	10	1.106	
0.4	2	0.771	3.660
	4	1.050	
	6	1.050	
	8	1.050	
	10	1.076	
tetrahedron distorted to icosahedral angles			
0	2	0.745	2.357
	4	0.745	
	6	1.660	
	8	0.745	
	10	1.102	
	<sup>a</sup>		
icosahedron-12			
0	2	0	4.871
	4	0	
	6	3.231	
	8	0	
	10	1.768	
0.1	2	0.463	4.076
	4	0.234	
	6	2.312	
	8	0.820	
	10	1.169	

Table 2. (continued)

mean square deviation	$l$	$Q_l$	normalization factor for 20 clusters
0.2	2	0.508	3.925
	4	0.701	
	6	1.551	
	8	1.070	
	10	1.167	
0.3	2	0.606	3.976
	4	1.048	
	6	1.157	
	8	1.055	
	10	1.132	
0.4	2	0.661	3.889
	4	1.055	
	6	1.098	
	8	1.103	
	10	1.081	

<sup>a</sup> Omissions due to limitations in space.

### Local Geometry in Liquid Argon

The configuration sets analysed were obtained by a grand canonical Monte Carlo simulation of argon, applying Lennard-Jones potentials.<sup>23</sup> The pair correlation function was in excellent agreement both with experiments and other simulations. Simulated thermodynamic parameters such as density, compressibility and heat capacity were also close to experimental data.

The size of the clusters was defined in two different ways: (i) by a cut-off sphere applied at a distance of 500 pm from the given central particle which, correspondingly, contained various numbers of neighbours giving an average of 12.0; (ii) by selecting only those clusters within the cut-off sphere which contained exactly 12 neighbours of the central particle. For case (i) we also made a distinction with respect to the energy of the central particle. The results are given in table 3 in which the mean square deviation of the invariants are also listed.

It is seen that the  $Q_l$  values of all cases in table 3, except the deepest-energy subset, coincide very well with the hexagonal close-packed ones randomized with a relative standard deviation of 0.1 to 0.3. On the other hand they significantly differ from those of icosahedral clusters. This also applies to the cases published by Steinhardt *et al.*, which correspond to simulations under different conditions.<sup>20</sup> The fact that both the distorted lattice and the individual cluster cases appear among the best fits of the reference systems (capital and lower case codes, respectively, in table 3) indicates that there may be some more or less extended regions of clusters aligned in a lattice-like way. This is supported by the finding of Steinhardt *et al.* that the distance correlation of  $Q_6$  extends beyond the size of a single cluster. Thus it can be concluded that, in the vicinity of its melting point, the structure of liquid argon consists of 13-particle clusters of the hexagonal close-packed arrangement which are not distorted beyond recognition.

This is an essentially different conclusion from that made in ref. (20), *viz.* that while liquid argon at  $T^* = 0.719$  and with reduced density of 0.973 is practically indistinguishable from a perfectly random system, the  $Q_l$  patterns of supercooled argon at  $T^* = 0.554$

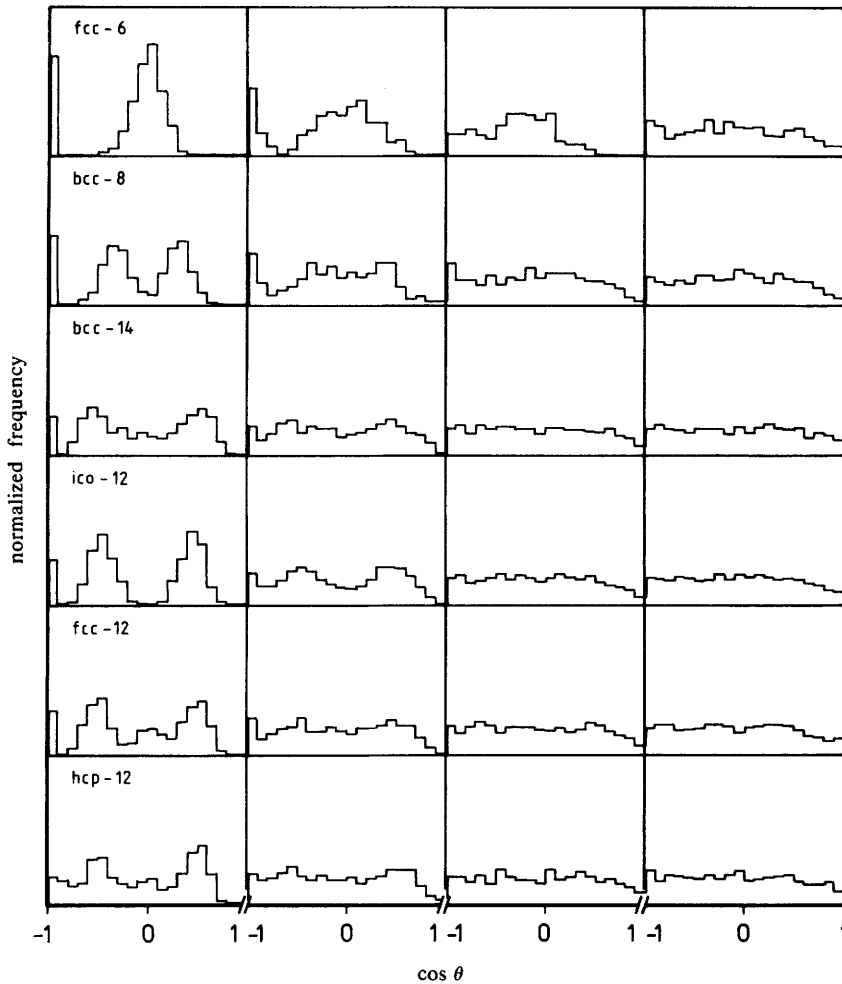


**Fig. 2.** The cosine distribution for various clusters. The degree of randomization is 0.1, 0.2, 0.3 and 0.4 from the left-1 to the right-hand side of the figure (see text).

suggests the possibility of icosahedral symmetry. We think that the authors, using unnormalized raw data, underestimated the significance of their results on normal liquid argon. On the other hand, since those results were not compared to gradually distorted regular clusters, it could be assumed that distortion of an icosahedron could yield the  $Q_i$  of supercooled argon which is, however, not the case.

While this seems to be generally true, it must be emphasized that the appearance of icosahedron as one of the possible structures just for the deepest-energy clusters (and as a ‘non-aligned’ one at that) shows that, at least in this partial case, the expectation of Steinhardt *et al.* is probably correct. In other aspects the energy dependence of the structure is almost unrecognizable in table 3. There seems to be a slight trend towards less distorted hexagonal close-packed units as the energy of the central particle decreases, but it is on the verge of insignificance.

Although the third-order invariants also characterize the angular correlation of ‘bonds’, they are much more sensitive to distortions, and thus uninformative in liquid

**Table 3.** Second- and third-order invariants of even- $l$  spherical harmonics for clusters with factor of renormalization  $f$ , (in brackets)

$l$	$Q_l$	standard deviation	$w_l \times 10^5$	standard deviation	symmetry/degree of randomization
$E > -650 K$ ( $f=19.3$ )					
2	0.482	0.316	-0.2	0.6	HCP-12/0.35
4	0.750	0.277	0.2	0.2	hcp-12/0.2
6	1.555	0.055	0	0.2	
8	1.240	0.021	0	0	
10	0.970	0.100	0	0	
$-650 > E/K > -700$ ( $f=19.7$ )					
2	0.543	0.176	0	0.6	HCP-12/0.4
4	0.774	0.291	0.3	0.4	fcc-12/0.2
6	1.387	0.269	-0.1	0	or
8	1.294	0.158	0	0	hcp-12/0.2
10	1.000	0.105	0	0.5	
$-700 > E/K > -750$ ( $f=30.5$ )					
2	0.436	0.009	-0.1	0.3	HCP-12/0.3
4	0.696	0.183	0	0	fcc-12/0.02
6	1.707	0.290	0	0	or
8	1.203	0.054	0	0.2	hcp-12/0.2
10	0.956	0.119	0	0	
$-750 > E/K > -800$ ( $f=31.5$ )					
2	0.428	0.108	0	0.1	HCP-12/0.3
4	0.609	0.047	0	0	hcp-12/0.1
6	1.947	0.393	0	0	
8	1.188	0.060	0	0	
10	0.825	0.152	0	0	
$-800 > E/K > -850$ ( $f=22.9$ )					
2	0.406	0.057	-0.3	0.1	HCP-12/0.3
4	0.613	0.022	0	0	hcp-12/0.1
6	1.783	0.625	0	0.1	
8	1.232	0.034	0.1	0.2	
10	0.963	0.025	0	0	
$-850K > E$ ( $f=11.6$ )					
2	0.360	0.128	-1.7	2.5	HCP-12/0.2
4	0.677	0.091	-0.5	3.1	or
6	1.615	0.059	-0.9	5.2	ICO-12/0.3
8	1.309	0.243	0.5	1.3	FCC-12/0.2
10	1.036	0.039	-0.1	0.2	hcp-12/0.1
$N=12$ ( $f=34.1$ )					
2	0.353	0.033	0	0	HCP-12/0.1
4	0.353	0.234	0	0	hcp-12/0.1
6	2.068	0.037	0	0	
8	1.331	0.193	0	0	
10	0.893	0.061	0	0	
all within cut-off ( $f=44.8$ )					
2	0.221	0.018	0	0.1	HCP-12/0.1
4	0.528	0.027	0	0	hcp-12/0.1
6	2.204	0.216	0	0	or
8	1.296	0.171	0	0	fcc-12/0.1
10	0.749	0.112	0	0	

argon under these conditions. As mentioned in the previous section, their non-zero values would indicate more or less extended four-body correlations.

### Local Structure in Molten Alkali-metal Halides

The second-order invariants of the spherical harmonics were also calculated for molten LiI and the complete set of molten alkali-metal chlorides simulated at temperatures slightly above their melting points under normal pressure. The configurations were obtained under conditions described elsewhere.<sup>26</sup> Since the third-order invariants proved to be less informative in the cases of other liquids covered in the present study, we omitted them, but included the calculation of the distance dependence of the second-order invariants instead.

The  $Q_l$  are listed in table 4. The conditions of selection, the formula of the molten salt, the charge sign of the central and neighbouring ions (+/- stands for both +/- and -/+) and the average number of neighbours within the cut-off sphere are given.

A general conclusion from these results is that the  $Q_l$  of the simulated configurations fit much better to some of the distorted lattice cases than to those of the individual clusters, *i.e.* these molten salts resemble the corresponding crystalline states not only in their first coordination spheres but in somewhat more extended (yet local) regions. Conclusions on the particular structures can be drawn as follows.

(i) There is the almost unanimous case of NaCl, KCl and CsCl, in which the geometry of the unlike-charged neighbours of the ions as well as both 'sublattices' of like-charged ones indicate the same structure. Indeed, one obtains an octahedral arrangement of unlike-charged neighbours when sliding two face-centred cubic sublattices into each other with a  $(\frac{1}{2}, 0, 0)$  shift of coordinates. RbCl has probably the same f.c.c. structure, although its cationic 'sublattice' seems to resemble a b.c.c. lattice rather than an f.c.c. one.

(ii) Similarly to the latter, the lithium salts represent cases when there seems to be some contradiction between the best-fitting structure of the total lattice and those of the 'sublattices'; however, the contradictions can be resolved. Namely, both  $\text{Li}^+$  and  $\text{I}^-$  subsystems show similarities to hexagonal close-packed lattices which, when interpenetrated to form a wurtzite-type structure, would require a tetrahedral +/- neighbourhood. The square planar structure, distorted at random, which gives the best fit, although not quite in harmony with this expectation, is not far from a tetrahedron distorted at random. The wurtzite-like structure of molten LiI is in excellent agreement with what has been concluded on the basis of the geometrical analysis of the same configurations by the Dirichlet-Voronoi polyhedra.<sup>19</sup> Similarly, with the interpenetration of the two b.c.c. lattices of LiCl one would expect to have a sphalerite-type tetrahedral structure; however, the best-fitting geometry of the +/- neighbours proved to be square planar or a deficient asymmetric octahedron. The lithium sublattices fit to more distorted cases than do the corresponding anion sublattices; this can be explained by the fact that these salts are weak superionic conductors in the solid state,<sup>27</sup> and the higher mobility of the small  $\text{Li}^+$  ions is preserved even in the molten state.

Fig. 3 (a) and (b) show the distance dependence of the  $Q_l$  on the two extreme examples of the f.c.c.-like structures of molten NaCl and CsCl. The curves, especially those of  $Q_8$  and  $Q_{10}$ , support the previous conclusion that the angular correlations extend beyond nearest-neighbour distances. The decay of distance correlation of the  $Q_l$  of NaCl is smooth, indicating less long-range correlation for  $Q_8(r)$  and  $Q_{10}(r)$ , whereas the same functions of CsCl (similar to KCl and RbCl) exhibit characteristic bumps for  $Q_6(r)$  and  $Q_8(r)$ . The fact that there are less particles within the first coordination sphere of the like-charged 'sublattices' of NaCl than in those of CsCl [*ca.* 14 and 18, respectively, as calculated by integrating to the first minimum in  $g_{++}(r)$  and  $g_{--}(r)$ ] is a consequence of the difference in the decay of the angular correlations.

**Table 4.** Second-order invariants of even- $l$  spherical harmonics for clusters in molten alkali-metal halides

selection	$l$	$Q_l$	symmetry/degree of randomization (renormalization factor)
LiI, +/-, $N = 3.9$	2	1.439	SQP-04/0.2 ( $f = 15.7$ )
	4	1.379	
	6	0.742	
	8	0.773	
	10	0.667	
LiCl, +/-, $N = 4.4$	2	0.896	FCC-04/0.4 or SQP-04/0.3 or sqp-04/0.2 ( $f = 16.3$ )
	4	1.531	
	6	0.733	
	8	0.977	
	10	0.863	
NaCl, ++, $N = 4.9$	2	0.540	FCC-06/0.3 ( $f = 18.0$ )
	4	2.104	
	6	0.899	
	8	0.809	
	10	0.647	
KCl, +/-, $N = 5.8$	2	0.474	FCC-06/0.2 ( $f = 16.3$ )
	4	2.451	
	6	0.817	
	8	0.768	
	10	0.490	
RbCl, +/-, $N = 5.7$	2	0.394	FCC-06/0.2 ( $f = 15.8$ )
	4	2.476	
	6	0.852	
	8	0.694	
	10	0.584	
CsCl, +/-, 6.0	2	0.342	FCC-06/0.2 ( $f = 10.7$ )
	4	2.671	
	6	0.833	
	8	0.726	
	10	0.427	
LiI, +/+, $N = 11.7$	2	0.396	HCP-12/0.3 or fcc-12/0.2 ( $f = 15.7$ )
	4	0.915	
	6	1.433	
	8	1.280	
	10	0.976	
LiCl, +/+, $N = 13.6$	2	0.500	BCC-14/0.3 or hcp-12/0.2 ( $f = 16.3$ )
	4	0.550	
	6	1.400	
	8	1.250	
	10	1.300	
NaCl, +/+, $N = 13.7$	2	0.391	FCC-18/0.3 or hcp-12/0.2 ( $f = 18.0$ )
	4	0.703	
	6	1.445	
	8	1.406	
	10	1.055	



Table 4. (continued)

selection	$l$	$Q_l$	symmetry/degree of randomization (renormalization factor)
KCl, +/+, $N = 16.6$	2	0.248	FCC-18/0.25
	4	0.496	or
	6	1.525	bcc-14/0.1
	8	1.950	( $f = 16.3$ )
	10	0.780	
RbCl, +/+, $N = 17.7$	2	0.484	BCC-14/0.3
	4	0.484	or
	6	1.694	bcc-14/0.1
	8	1.371	( $f = 15.8$ )
	10	0.968	
CsCl, +/+, $N = 18.0$	2	0.211	FCC-18/0.05
	4	0.282	( $f = 10.7$ )
	6	1.056	
	8	2.570	
	10	0.880	
LiI, -/-, $N = 11.8$	2	0.433	HCP-12/0.2
	4	0.793	( $f = 15.7$ )
	6	2.067	
	8	0.986	
	10	0.721	
LiCl, -/-, $N = 13.8$	2	0.231	BCC-14/0.2
	4	0.692	or
	6	1.846	bcc-14/0.1
	8	1.115	or
	10	1.115	hcp-12/0.1 ( $f = 16.3$ )
NaCl, -/-, $N = 14.3$	2	0.685	fcc-18/0.2
	4	0.444	( $f = 18.0$ )
	6	1.290	
	8	1.532	
	10	1.048	
KCl, -/-, $N = 17.0$	2	0.203	FCC-18/0.1
	4	0.291	( $f = 16.3$ )
	6	1.221	
	8	2.209	
	10	1.076	
RbCl, -/-, $N = 17.4$	2	0.543	FCC-18/0.2
	4	0.775	( $f = 15.8$ )
	6	1.008	
	8	1.434	
	10	1.240	
CsCl, -/-, $N = 18.6$	2	0.284	FCC-18/0.1
	4	0.483	( $f = 10.7$ )
	6	1.080	
	8	2.528	
	10	0.625	

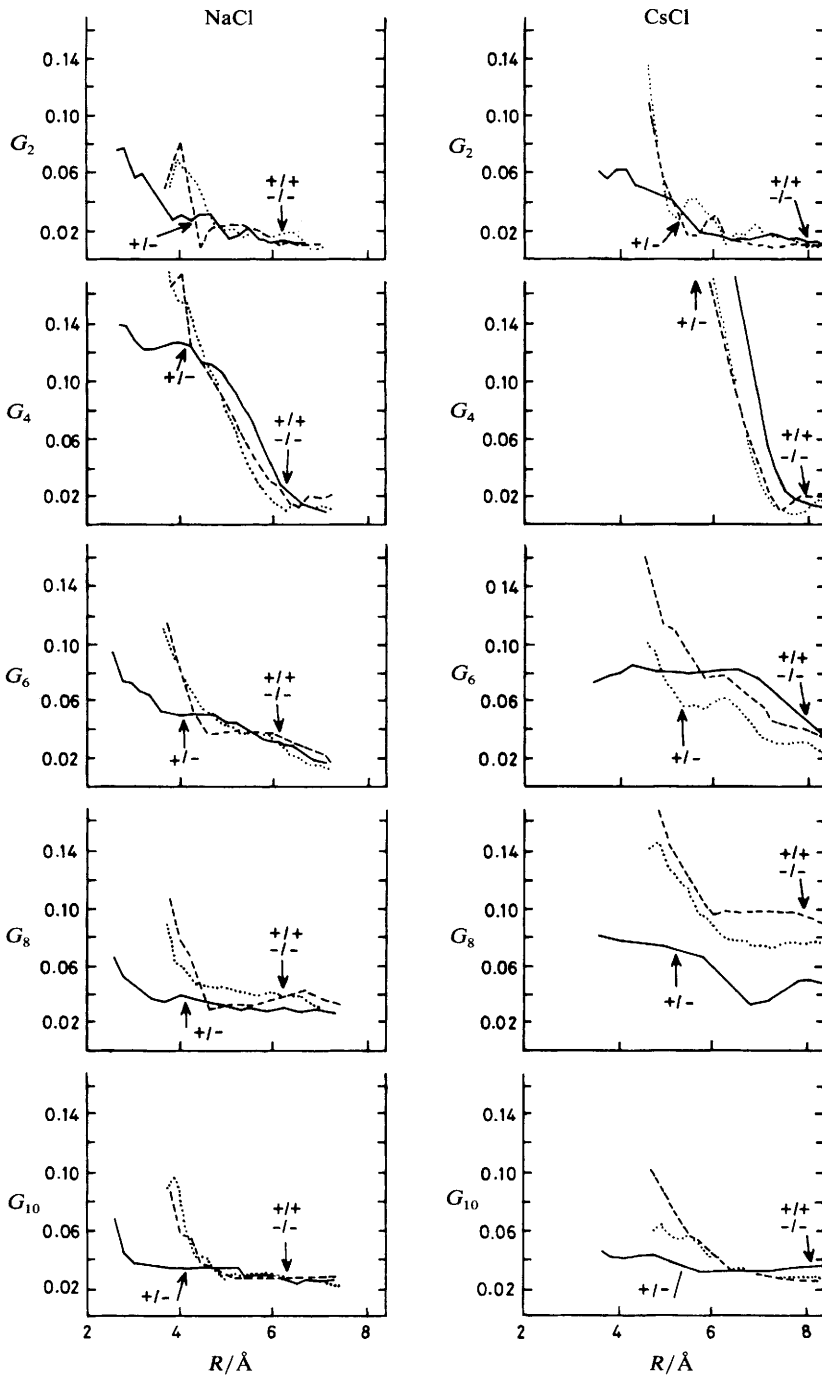


**Fig. 3.** (a) Dependence of the even- $l$  rotational invariants on the distance of the middle point of bond vectors from the central particle in molten NaCl. Arrows with +/-, +/+ and -/- signs show the cut-off radius used in calculating the data in table 4. The curves are taken only within the minimum image box. (b) As (a) but for molten CsCl.

The symmetry of the clusters corresponds to lattices which are the stable crystalline states under normal pressure, except for the cases of molten LiI and LiCl, which should also be f.c.c.-like, instead of having the wurtzite- or sphalerite-like structure indicated by the invariants. The strong resemblance of the f.c.c. lattice of the molten sodium, potassium, rubidium and caesium chlorides near their melting points is probably the reason why there are no reports of their forming glasses.<sup>28</sup> The geometrical differences of the lithium halides in their molten and crystalline states may partly explain why their melting points are depressed much lower than those of the sodium halides.

### Local Structure in Water

The application of the rotational invariants of spherical harmonics to discover local order in simulated water samples has been much less successful than in the cases discussed above.

20 independent configurations of liquid water simulated by the molecular-dynamics method<sup>29</sup> at room temperature and under normal pressure using ST2 pair potentials<sup>30</sup> were analysed with respect to the positions of the oxygen atoms. The simulation box contained 200 water molecules. The results are summarised in table 5, together with those obtained on a sample of a low-density ( $0.8 \text{ cm}^{-3}$ ) fictitious model of water.<sup>31</sup>

In contrast to expectations based on the assumption of extended hydrogen-bonded structure, normal water seems to be disordered, at least as far as the nearest neighbourhood is considered. Except for the  $Q_2$ , practically all the  $Q_l$  are equal to unity within standard deviations. Similarly, all the  $w_l$  are very close to zero. Taking into account, however, that on one hand, the reference values of the invariants for the undistorted clusters themselves (see tables 1 and 2) are not far from unity and, on the other hand, that they approach unity quite rapidly with randomization, it can also be concluded that the invariants are less sensitive to local symmetries than they are for larger clusters. Thus the loose structure of water with a low coordination number for the water molecules is not a good field of application of the spherical harmonic invariants.

In light of this it is the more striking that the 'low-pressure' water seems to be so structured, although the extent of the network of hydrogen bonds had been known to be greater than that in normal water.<sup>31</sup> We have been unsuccessful in finding the cluster which would correspond exactly to the values of  $Q_l$  obtained as averages of 40 independent configurations of 216 water molecules. It is doubtless, however, that no angular correlations of four nearest neighbours can yield these values, neither can any simple combination of random distorted tetrahedra. The low value of  $Q_8$  and  $Q_{10}$  can be achieved by 'double' icosahedral angles (see fig. 4) between several pairs of bond vectors within or in between the five-membered basic clusters, but the simultaneously high value of  $Q_6$  can be attained only by some peculiar arrangement of the 'tetrahedra distorted to icosahedral angles'. The invariance of the  $Q_l$  data with respect to the number of neighbours considered is another proof of the existence of rather large clusters. After several trials and errors, the cluster depicted in fig. 5 gave  $Q_l$  patterns similar to the values obtained on low-pressure water.

In the search for the appropriate cluster, we have utilized a recent result of Pálínkás *et al.*<sup>32</sup> who found by statistics on the first coordination spheres of water molecules in both ST2 and 'central force' models that the distance between two molecules in the coordination sphere is the same as that between them and the central molecule. That is, three water molecules form an approximately regular triangle. If one assumes that the other two neighbours in the first coordination sphere open up the angle between them to make it identical with that between one of their bond and either of those that closed up to each other, then this optimum angle proves to be *ca.*  $117^\circ$ . In comparison to this, the 'double' icosahedral angle is  $116.65^\circ$ , which is in excellent agreement with the former value.

**Table 5.** Second- and third-order invariants of even- $l$  spherical harmonics for clusters in ST2 model water conditions of selection shown, with factor of renormalization,  $f$ , in brackets

1	$Q_l$	standard deviation	$w_l \times 10^5$	standard deviation	symmetry/degree of randomization
'normal' water					
first 2 neighbours ( $f = 16.4$ )					
2	0.788	0.239	0.7	0.4	dia-02/ < .2
4	1.068	0.252	0.2	0.9	
6	1.119	0.172	0	0	
8	1.004	0.119	0	0	
10	1.019	0.116	0.1	0	
first 3 neighbours ( $f = 19.5$ )					
2	0.680	0.198	0.3	0.7	dia-03/ > 0.1
4	1.103	0.296	0	0.1	or
6	1.130	0.179	0	0.1	trp-03/0.3
8	1.013	0.161	0	0.3	
10	1.072	0.103	0	0	
first 4 neighbours ( $f = 22.0$ )					
2	0.606	0.171	0.1	1.2	ico-04/0.2
4	1.137	0.324	0	0	or
6	1.161	0.165	0	0.1	dia-04/ > 0.3
8	1.007	0.171	0	0.1	fcc-04/0.3
10	1.086	0.070	0	0	trp-04/ > 0.2
first 5 neighbours ( $f = 31.4$ )					
2	0.471	0.377	0	0	tbp-05/ > 0.2
4	1.132	0.169	0	0	or
6	1.163	0.206	0	0	dia-05/ > 0.2
8	1.226	0.206	0	0	
10	1.006	0.149	0	0	
first 6 neighbours ( $f = 27.1$ )					
2	0.545	0.301	0.1	0.5	fcc-06/ > 0.3
4	1.053	0.336	0	0.2	
6	1.199	0.236	0	0	any
8	1.164	0.203	0	0	dia-06/0.3
10	1.036	0.130	0	0	
all within 0.34 nm ( $f = 24.4$ )					
2	0.539	0.187	0.7	0.7	trp-04/0.1
4	1.073	0.309	0	0.2	or
6	1.265	0.180	0	0.1	dia-04/0.3
8	1.095	0.185	0	0.1	
10	1.026	0.112	0	0	
'low-pressure' water					
first 2 neighbours ( $f = 3.39$ )					
2	1.303	0.010	16.4	3.4	fig. 6/ < 0.1
4	0.434	0.075	131.1	32.3	
6	2.771	0.573	-67.9	18.5	
8	0.234	0.034	23.8	8.5	
10	0.258	0.037	-2.6	26.1	
first 3 neighbours ( $f = 3.52$ )					
2	1.333	0.032	3.2	3.9	fig. 6/ < 0.1
4	0.445	0.042	125.4	31.3	
6	2.800	0.470	-74.3	12.5	

Table 5. (continued)

1	$Q_l$	standard deviation	$w_l \times 10^5$	standard deviation	symmetry/degree of randomization
8	0.200	0.024	36.6	20.6	
10	0.221	0.032	-4.4	44.7	
first 4 neighbours ( $f=3.64$ )					
2	1.403	0.022	-33.1	12.2	fig. 6/ <0.1
4	0.430	0.029	103.7		
6	2.759	0.448	-73.3	6.8	
8	0.203	0.022	45.9	14.3	
10	0.215	0.029	-3.0	49.4	
first 5 neighbours ( $f=3.64$ )					
2	1.395	0.022	-27.3	10.1	fig. 6/ <0.1
4	0.435	0.033	96.3	45.8	
6	2.765	0.464	-72.0	7.4	
8	0.194	0.022	45.4	20.3	
10	0.212	0.029	-3.3	49.3	
first 6 neighbours ( $f=3.65$ )					
2	1.394	0.022	-28.6	11.3	fig. 6/ <0.1
4	0.434	0.033	94.2	48.5	
6	2.766	0.456	-71.8	7.2	
8	0.193	0.022	45.9	20.4	
10	0.212	0.026	-3.5	52.7	
all within 0.34 nm ( $f=3.65$ )					
2	1.395	0.023	-28.3	11.4	fig. 6/ <0.1
4	0.433	0.031	94.0	48.5	
6	2.853	0.456	-71.9	7.2	
8	0.193	0.024	45.9	20.4	
10	0.211	0.027	-3.5	52.7	

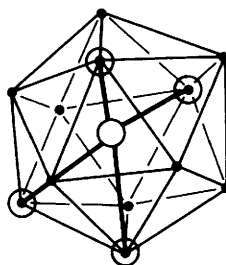


Fig. 4. The distorted tetrahedron of the most likely arrangement of five nearest-neighbour water molecules placed into an icosahedron.

However, the reason for this peculiar distortion of the tetrahedra is still a puzzle to us, and we plan to study it by including the angular correlations within the subsystem of protons as well as between oxygens and protons.

### Conclusions

In light of the previous sections, the rotational invariants of even- $l$  spherical harmonics can be utilized in characterizing the angular correlations within or in between clusters

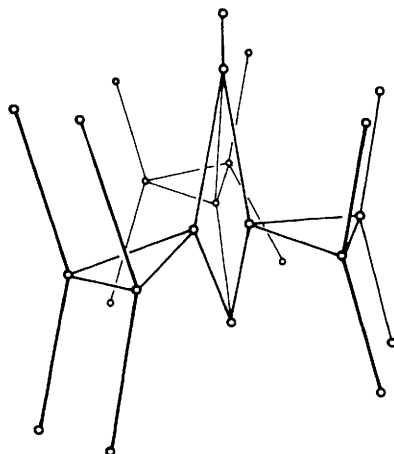


Fig. 5. A schematic perspective representation of the 24-molecule cluster of 'low-pressure' water.

of particles in fluids. The second- and third-order invariants represent three- and four-body angular correlations. The values of the  $w_i$  seem to be too sensitive to small changes in the geometry of the clusters in liquids; therefore they tend rapidly to zero as the degree of randomization increases. The second-order invariants retain their characteristic features even in rather disordered systems. Thus, they are more suitable to detect residual symmetry properties in the geometry of clusters than either the third-order invariants or the distribution function of angles formed by pairs of bond vectors. This is because the relationship of these invariants to the angular distribution function is similar to that of the moments of a probability density to the corresponding distribution in such a way that the evenly distributed noise does not contribute to the values of the invariants. Therefore, the  $Q_l$  have the optimum sensitivity as indicators of local order in fluids.

By choosing the appropriate method of renormalization to eliminate the effect of sample size on the values of the invariants and by using a set of reference values to which the invariants of a configuration under study are compared, information can be obtained on symmetry properties of local clusters as well as eventual inter-cluster angular correlations. Although the odd- $l$  invariants, calculated from spherical harmonics averaged over all bonds, are expected to be zero owing to the isotropic nature of fluids, they may be non-zero, and thus serve as additional order parameters, if the averages are taken only within adjacent neighbourhoods, i.e. if only intra-cluster correlations are to be revealed. This aspect deserves further attention.

It would also be appropriate to investigate the eventual effects of the size of the simulation box on the value of the rotational invariants. Although we do not expect such effects to bias the data, they may be significant in studies of long-range correlations (owing to long-range forces) in an insufficiently sized simulation box.

The structure of dense liquids, such as Lennard-Jones argon and the simple Coulomb liquids represented in this study by the molten alkali-metal halides, is determined mainly by the repulsion potentials acting among the particles, i.e. by their size. This seems to be the governing rule beyond the facts that (i) argon has a local hexagonal close-packed structure, (ii) molten sodium, potassium, rubidium and caesium chlorides have face-centred cubic lattice-like, non-local structures in increasing extent in this order, and (iii) molten lithium chloride and iodide have sphalerite- and wurtzite-type lattice-like structures. All of these correspond to expectations based on models of best-fitting spheres.

The structure-making effect of angle-dependent attraction forces seem to predominate in low-density liquids such as 'low-pressure' water, whereas the same pair potentials cannot build up such an extended hydrogen-bonded structure when the density is slightly increased from its optimum with respect to hydrogen bonding although retaining the low density relative to the above examples of liquid argon and molten salts. Thus liquid water under normal pressure and temperature seems to be the most disordered liquid among those studied in this paper as far as local geometry is concerned.

## References

- 1 (a) B. J. Ackerson, T. W. Taylor and N. A. Clark, *Phys. Rev. A*, 1985, **31**, 3183; (b) B. J. Ackerson, T. W. Taylor and N. A. Clark, *J. Phys. (Paris)*, 1986, **46**, 137.
- 2 F. H. Stillinger and T. A. Weber, *Kinam*, 1981, **3A**, 159.
- 3 F. H. Stillinger and T. A. Weber, *Phys. Rev.*, 1982, **25**, 978.
- 4 F. H. Stillinger and T. A. Weber, *J. Phys. Chem.*, 1983, **87**, 2833.
- 5 F. H. Stillinger and T. A. Weber, *J. Chem. Phys.*, 1984, **80**, 4434.
- 6 T. A. Weber and F. H. Stillinger, *J. Chem. Phys.*, 1984, **81**, 5089.
- 7 F. H. Stillinger and T. A. Weber, *Science*, 1984, **225**, 983.
- 8 T. A. Weber and F. H. Stillinger, *Phys. Rev.*, 1985, **32**, 5402.
- 9 F. H. Stillinger and R. A. LaViolette, *J. Chem. Phys.*, 1985, **83**, 6413.
- 10 G. L. Dirichlet, *J. Reine Angew. Math.*, 1850, **40**, 216.
- 11 G. F. Voronoi, *J. Reine Angew. Math.*, 1908 **134**, 199.
- 12 J. L. Finney, *Proc. R. Soc. London, Ser. A*, 1970, **139**, 479.
- 13 B. J. Gellatly and J. L. Finney, *J. Non-Cryst. Solids*, 1982, **50**, 313.
- 14 A. Rahman, M. J. Mandell and J. P. McTeague, *J. Chem. Phys.*, 1976, **64**, 1564.
- 15 M. J. Mandell, J. P. Teague and A. Rahman, *J. Chem. Phys.*, 1976, **64**, 3699; 1977, **66**, 3070.
- 16 M. Tanemura, Y. Hiwatari, H. Matsuda, T. Ogawa, N. Ogita and A. Ueda, *Prog. Theor. Phys.*, 1977, **58**, 1079; 1978, **59**, 323.
- 17 J. Neil Cape, J. L. Finney and L. V. Woodcock, *J. Chem. Phys.*, 1981, **75**, 2366.
- 18 E. E. David and C. W. David, *J. Chem. Phys.*, 1982, **76**, 4611.
- 19 A. Baranyai and I. Ruff, *J. Chem. Phys.*, 1986, **85**, 365.
- 20 P. J. Steinhardt, D. R. Nelson and M. Ronchetti, *Phys. Rev. B*, 1983, **28**, 784.
- 21 L. D. Landau and E. M. Lifschitz, *Statistical Physics*, Pergamon Press, London, Chapter XIV.
- 22 S. Nosé and F. Yonezawa, *Solid State Commun.*, 1985, **56**, 1005; 1009.
- 23 I. Ruff, A. Baranyai, G. Pálinkás and K. Heinzinger, *J. Chem. Phys.*, 1986, **85**, 2169.
- 24 L. D. Landau and E. M. Lifschitz, *Quantum Mechanics* (Hungarian translation), (*Műszaki Kiadó, Budapest*, 1978), mathematical supplement.
- 25 I. S. Gradstein and I. M. Rizhik, *Tablicy Integralov, Summ, Ryadov i Proizvodenii* (Nauka, Moscow, 1971), p. 1027.
- 26 A. Baranyai, I. Ruff and R. L. McGreevy, *J. Phys. C*, 1986, **19**, 453.
- 27 M. Menetrier, A. Levasseur, C. Delmas, J. F. Audebert and P. Hagenmuller, *Solid State Ionics*, 1984, **14**, 257; E. Schreck, K. Lägernd, and K. Dransfeld, *Z. Phys., Teil B*, 1986, **62**, 331; R. L. McGreevy, personal communication.
- 29 G. I. Szász, K. Heinzinger and W. O. Riede, *Z. Naturforsch., Teil A*, 1981, **36**, 1067.
- 30 F. H. Stillinger and A. Rahman, *J. Chem. Phys.*, 1970, **60**, 1545.
- 31 A. Geiger, P. Mausbach and J. Schnitker, in *Water and Aqueous Solutions*, ed. G. W. Nelson and J. E. Enderby, Bristol, 1986, in press; A. Geiger, P. Mausbach, J. Schnitker, R. L. Blumberg and H. E. Stanley, *J. Phys (Paris), Suppl.*, **45**, C7-13.
- 32 Pálinkás, P. Bopp, G. Jancsó and K. Heinzinger, *Z. Naturforsch., Teil A*, 1983, **39**, 179.